Nowak, A.S., Kim, S. "Weigh-in-Motion Measurement of Trucks on Bridges."
Bridge Engineering Handbook.
Ed. Wai-Fah Chen and Lian Duan
Boca Raton: CRC Press, 2000

55

Weigh-in-Motion Measurement of Trucks on Bridges

Andrzej S. Nowak
University of Michigan

Sangjin Kim
Kyungpook National University, Korea

55.1 Introduction

Knowledge of the past and current load spectra, together with predicted future loads, is essential in the evaluation and fatigue analysis of existing bridges. Many trucks carry loads in excess of design limits. This may lead to fatigue failure. The information concerning actual load is very important for the rating of bridges. Therefore, there is a need for accurate and inexpensive methods to determine the actual loads, the strength of the bridge, and its remaining life. There is also a need for verification of live load used for the development of a new generation of bridge design codes [1,2]. It has been confirmed that truck loads are strongly site specific [3,4,5]. Some bridges carry heavy truck traffic (volume and magnitude); others carry only lighter traffic. Furthermore, load effects such as bending moment, shear, and/or stress are component specific [6,7]. This observation is important in evaluation of the fatigue damage and prediction of remaining life. This chapter presents some of the practical procedures used for field measurement of truck weights and resulting strains.

55.2 Weigh-in-Motion Truck Weight Measurement

55.2.1 Weigh-in-Motion Equipment

The bridge live load is the load caused by truck traffic. In the past, truck data were collected by truck surveys, which had limitations. The most common survey method consisted of weighing trucks using static scales installed in weigh stations at fixed locations along major highways. The usefulness of the data obtained, however, is limited because many drivers of overloaded trucks intentionally avoid the scales, and therefore the results are biased to lighter trucks.

Therefore, research effort was focused on developing weigh-in-motion (WIM) methodology which can provide unbiased truck data, including axle weight, axle spacing, vehicle speed, multiple presence of trucks, and average daily truck traffic (ADTT). Very good results were obtained by using a WIM system with a bridge as a scale. Sensors measure strains in girders, and this is used to calculate the truck parameters at the highway speed.

The WIM system provides instrumentation invisible to truck drivers, and, therefore, the drivers do not try to avoid the scale. The system is portable and can be easily installed on a bridge to obtain site-specific truck data.

The bridge WIM system consists of three basic components: strain transducers, axle detectors (tape switches or infrared sensors), and data acquisition and processing system (Figure 55.1). The analog front end (AFE) acts as a signal conditioner and amplifier with a capacity of eight input channels. Each channel can condition and amplify signals from strain transducers. During data acquisition, the AFE maintains the strain signals at zero. The autobalancing of the strain transducers is activated when the first axle of the vehicle crosses the first axle detector. As the truck crosses the axle detectors the speed and axle spacing are determined. When the vehicle enters the bridge, the strain sampling is activated. As the last axle of the vehicle has exited the instrumented bridge span, the strain sampling is turned off. Data received from strain transducers are digitized and sent to the computer where axle weights are determined by an influence line algorithm. These data do not include dynamic loads. This process takes from 1.5 to 3.0 s, depending on the instrumented span length, vehicle length, number of axles, and speed. The data are then saved to memory.

The WIM equipment is calibrated using calibration trucks. The readings are verified and calibration constants are determined by running a truck with known axle loads over the bridge several times in each lane. The comparison of the results indicates that the accuracy of measurements is within 13% for 11-axle trucks. Gross vehicle weight (GVW) accuracy for five-axle trucks is within 5%, however, the accuracy is within 20% for axle loads [5].

55.2.2 Testing Procedure

The WIM system provides truck axle weights, gross vehicle weights, and axle spacings. Strains are measured in lower flanges of the girders and the strain time history is decomposed using influence lines to determine vehicle axle weights, as shown in Figure 55.1. The strain transducer can be clamped to the upper or lower surface of the bottom flange of the steel girder as shown in Figure 55.2. All transducers are placed on the girders at the same distance from the abutment, in the middle third of a simple span. The vehicle speed, time of arrival, and lane of travel are obtained using lane sensors on the roadway placed before the instrumented span of the bridge (Figure 55.3).

Two types of lane sensors can be used depending on the site conditions: tape switches and infrared sensors. Tape switches consist of two metallic strips that are held out of contact in the normal condition. As a vehicle wheel passes over the tape it forces the metallic strips into contact and grounds a switch. If a voltage is impressed across the switch, a signal is obtained at the instant the vehicle crosses the tape. This signal is fed to a computer whereby the speed, axle spacing, and number of axles are determined. The tape switches are placed perpendicular to the traffic flow and used to trigger the strain data collection. All cables used to connect tape switches and strain transducer to the AFE are five-pin wire cables.

The major problem with tape switches is their vulnerability to damage by moving traffic, particularly if the pavement is wet. Various alternative devices can be considered. Infrared sensors can be used to replace the tape switches. The infrared system consists of a source of infrared light beam and a reflector. The light source is installed on the side of the road. The reflector is installed in the center of the traffic lane. However, the problem of their vulnerability to damage by moving traffic has not been resolved. The infrared system is more difficult to install and trucks can easily move the reflector and interrupt the operation (the light beam must be aligned).

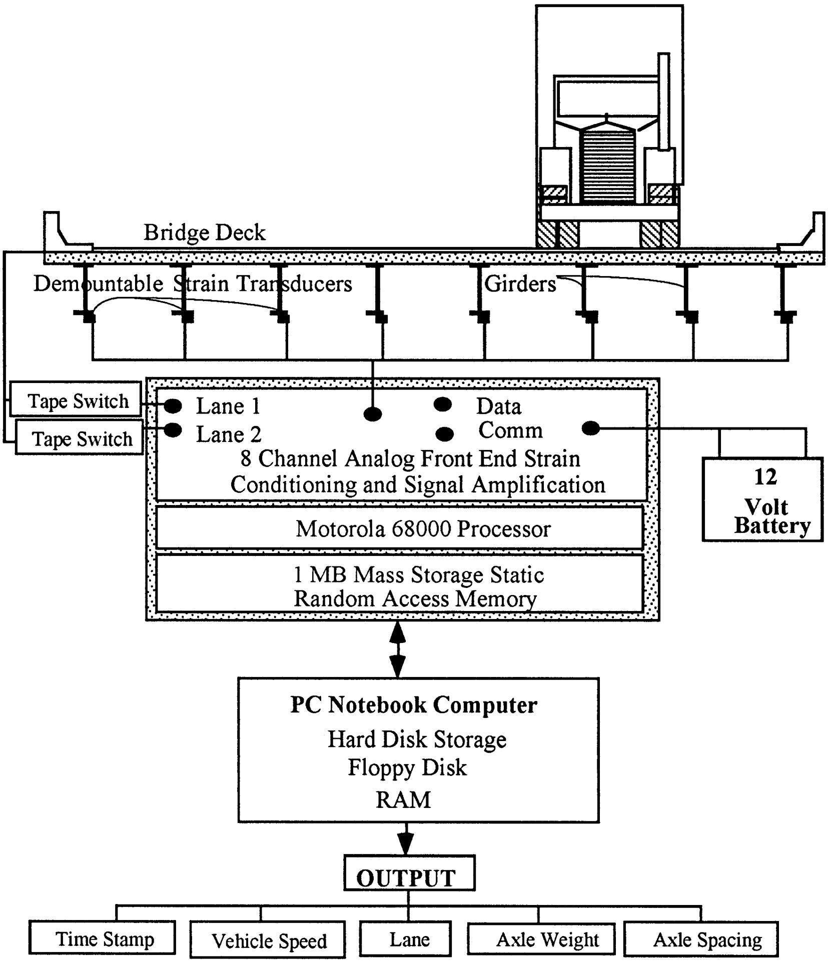

FIGURE 55.1 WIM truck measurement system.

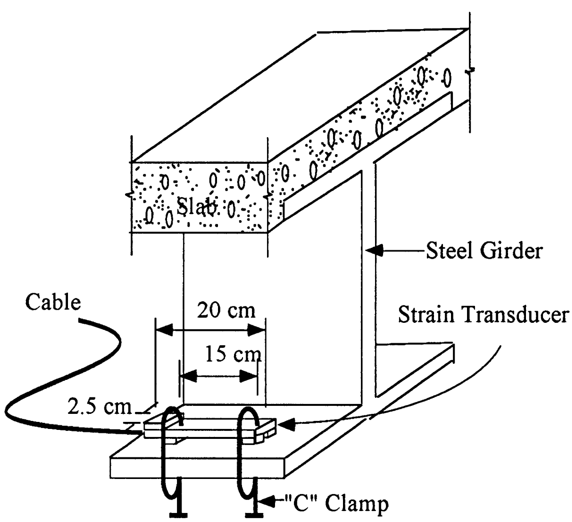

FIGURE 55.2 Demountable strain transducer mounted to the lower flange.

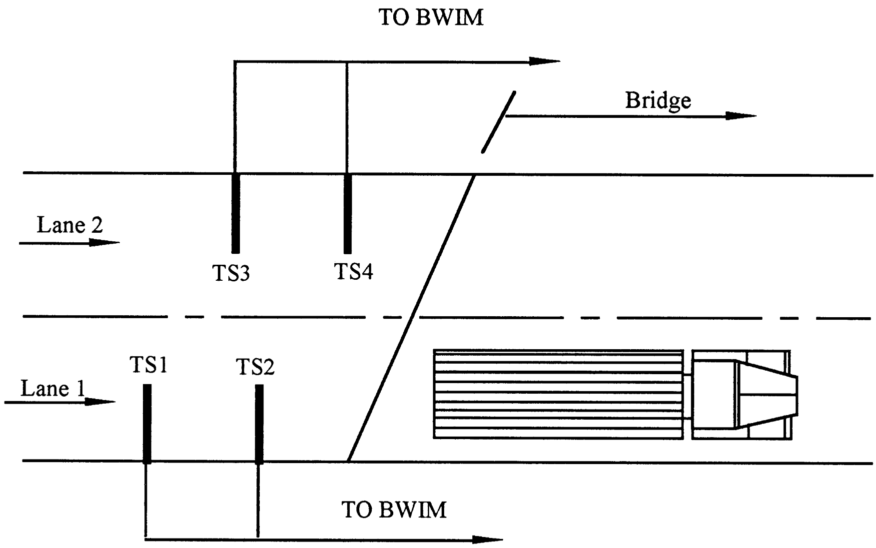

FIGURE 55.3 Plan of roadway sensor configuration.

TABLE 55.1 Parameters of Selected Bridges

Bridge Location	Span (m)	Number of Girders	Girder Spacing (m)	Number of Lanes	ADTT (One Direction)
WY/I-94	10.0	9	1.55	2	750
I-94/M-10	23.2	5	2.70	2	1,500
U.S. 12/I-94	12.0	9	1.68	2	500
DA/M-10	13.1	8	1.57	2	750
M-39/M-10	10.0	8	1.85	3	1,500
I-94/I-75	13.5	8	1.40	2	1,500
M-153/M-39	9.5	12	1.75	3	500

55.2.3 Selection of Bridges for Testing

The WIM measurements are demonstrated on seven bridges [3–5]. The selected structures are located in Michigan. Important factors considered in the selection process included accessibility from the ground, availability of space to work, low dynamic effects, and placement of tape switches or infrared sensors. The basic parameters are listed in Table 55.1. They include span length, number of girders, girder spacing, number of traffic lanes, and ADTT. ADTT was estimated on the basis of truck measurements performed for this study and it varies from 500 to 1500 in one direction. Bridge location is denoted by intersection of two roads; the first symbol stands for the road carried by the bridge, and the other one indicates the road under the bridge. Spans vary from about 10 to 25 m. The traffic volume is expressed in terms of ADTT. The selected bridges represent typical structures. The elevation and cross section of a typical bridge are shown in Figure 55.4.

55.2.4 Results from WIM Tests

55.2.4.1 Gross Vehicle Weight Distributions

The WIM results can be presented in a form of a traditional histogram (frequency or cumulative). However, this approach does not allow for an efficient analysis of the extreme values (upper or lower tails) of the considered distribution. Therefore, results of GVW WIM measurements for seven bridges are shown in Figure 55.5 in the form of cumulative distribution functions (CDFs) on the

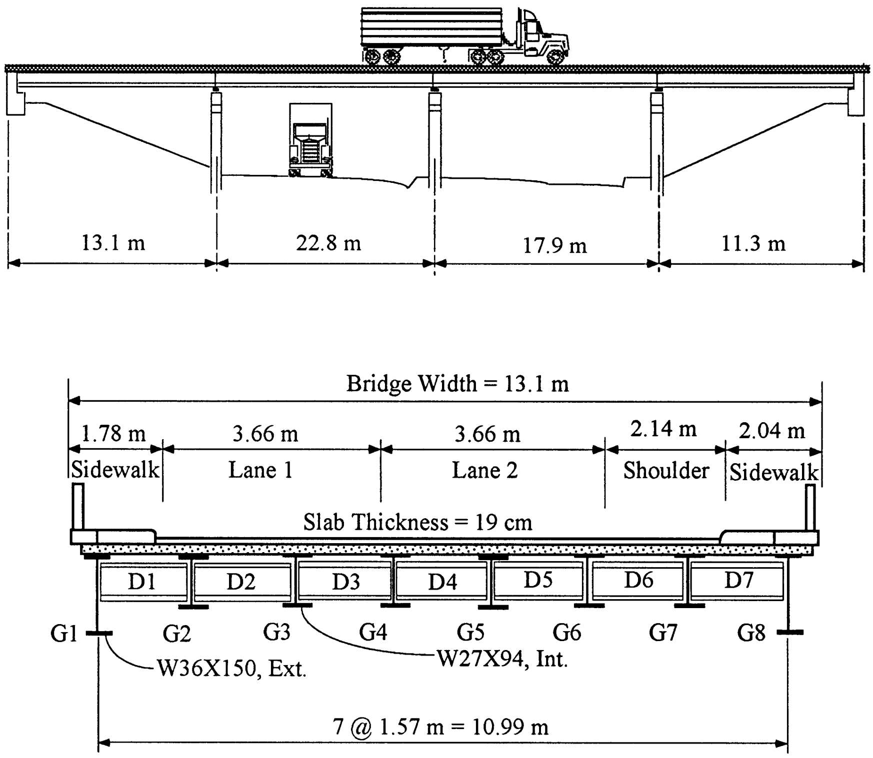

FIGURE 55.4 Bridge DA/M-10.

normal probability paper. CDFs are used to present and compare the critical extreme values of the data. They are plotted on normal probability paper [8]. The horizontal scale is in terms of the considered truck parameter (e.g., GVW, axle weight, lane moment, or shear force). The vertical scale represents the probability of being exceeded, p. Then, the probability of being exceeded (vertical scale) is replaced with the inverse standard normal distribution function, $\Phi^{-1}(p)$. For example, $\Phi^{-1}(p) = 0$, corresponds to the probability of being exceeded, $p = 0.5$; $\Phi^{-1}(p) = 1$, corresponds to $p = 0.159$; and $\Phi^{-1}(p) = -1$ corresponds to $p = 0.841$; and so on.

The distribution of truck type by number of axles will typically bear a direct relationship to the GVW distribution; the larger the population of multiple-axle vehicles (greater than five axles) the greater the GVW load spectra. Past research has indicated that 92 to 98% of trucks are four- and five-axle vehicles. The data obtained in this study indicate that between 40 and 80% of the truck population are five-axle vehicles, depending considerably on the location of the bridge. Three- and four-axle vehicles are often configured similarly to five-axle vehicles, and when included with five-axle vehicles account for between 55 and 95% of the truck population. Between 0 and 7.4% of the trucks are 11-axle vehicles in Michigan.

Most states in the United States allow a maximum GVW of 355 kN where up to five axles per vehicle are permitted. The State of Michigan legal limit allows for an 11-axle truck of up to 730 kN, depending on axle configuration. There were a number of illegally loaded trucks measured during data collection at several of the sites. Maximum WIM truck weights (1192 kN) exceeded legal limits by as much as 63%.

55.2.4.2 Axle Weight Distributions

Potentially more important for bridge fatigue and pavement design are the axle weights and spacing for trucks passing over the bridge. Figure 55.6 presents the distributions of the axle weights of the measured vehicles. All distributions include axles with weights greater than 22 kN. The maximum axle weights vary from 90 to 225 kN, and average values from 30 kN to 60 kN.

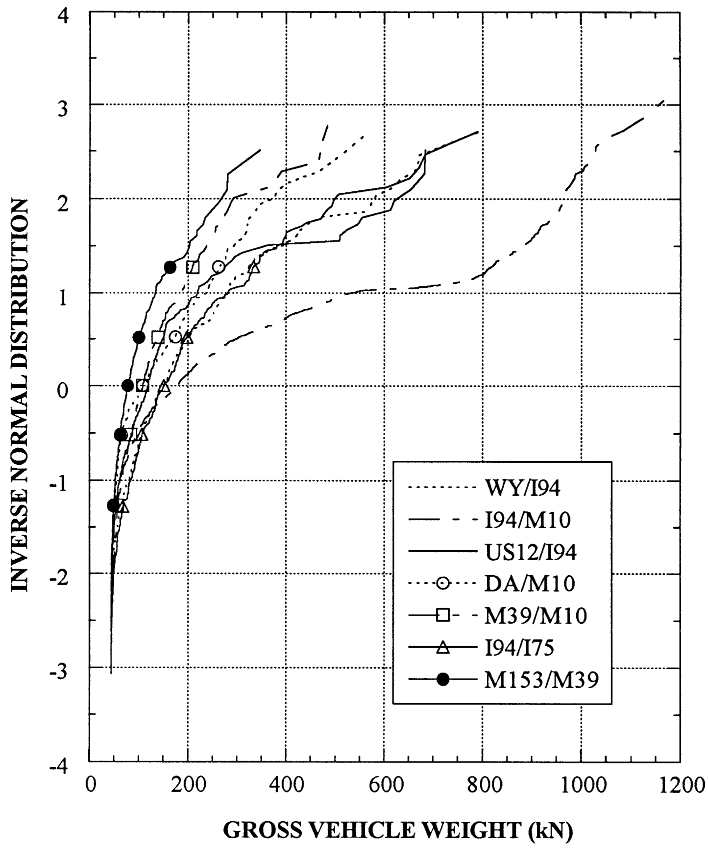

FIGURE 55.5 CDFs of GVW for the considered bridges.

55.2.4.3 Lane Moment and Shear Distributions

The structure is affected by load effects. Therefore, for the measured trucks, lane moments and shears were calculated for various spans. The resulting CDFs for 27-m span are shown in Figure 55.7 for lane moment and Figure 55.8 for lane shear. Each truck in the database is analytically driven across the bridge to determine the maximum static bending moment (shear) per lane. The CDFs of the lane moments (shears) for a span of 27 m are then determined. As a point of reference, the calculated moments (shears) are divided by design moment (shear) specified by the new AASHTO LRFD Specification [1]. The design live load according to the AASHTO LRFD is a superposition of a truck weighing 320 kN (three axles: 35, 145, and 145 kN spaced 4.25 m) and a uniformly distributed load of 9.3 kN/m. The lane moments in Figure 55.7 show a wide variation among bridges. Maximum values of the ratio of lane moment to LRFD moment vary from 0.6 at M-153/M-39 to 2.0 at I-94/M-10. All sites have a median lane moment between 0.16 and 0.34 times LRFD moment, which corresponds to an inverse normal value of 0. The variation of lane shears in Figure 55.8 is similar to that of lane moments. For I-94/M-10, the extreme value exceeds 2.0. For other bridges, the maximum shears vary from 0.65 at M-153/M-39 to 1.5 at I-94/I-75.

55.3 Fatigue Load Measurement

55.3.1 Testing Equipment

The Stress Measuring System (SMS) with the main unit manufactured by the SoMat Corporation is shown in Figure 55.9. The SMS compiles stress histograms for the girders and other components.

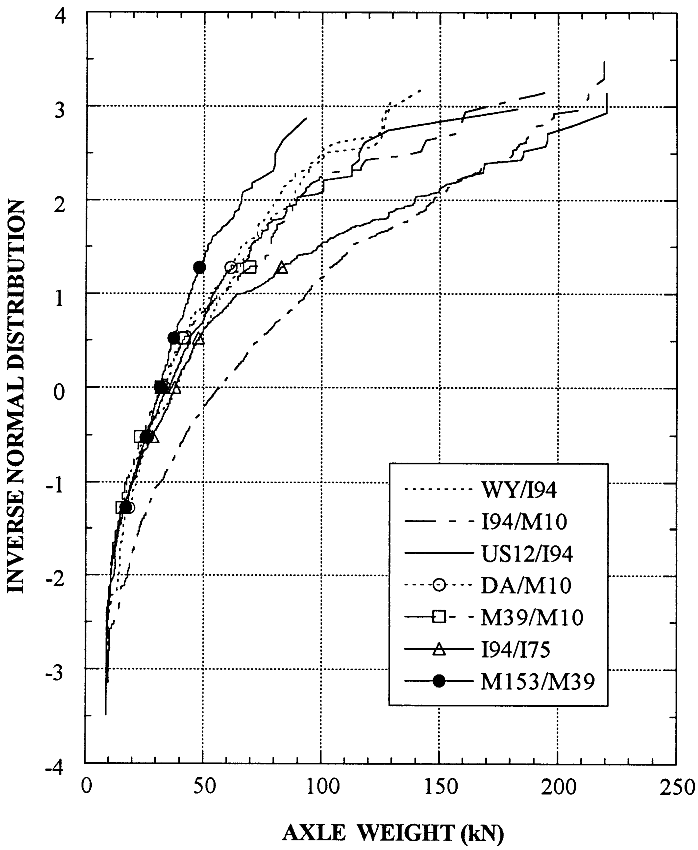

FIGURE 55.6 CDFs of axle weight for the considered bridges.

The SMS collects the strain history under normal traffic and assembles the stress cycle histogram by the rainflow method of cycle counting, and other counting methods. The data are then stored to memory and downloaded at the conclusion of the test period. The rainflow method counts the number, n, of cycles in each predetermined stress range, S_i, for a given stress history. The SMS is capable of recording up to 4 billion cycles per channel for extended periods in an unattended mode. Strain transducers were attached to all girders at the lower, midspan flanges of a bridge. Dynamic strain cycles were measured under normal traffic using the rainflow algorithm.

The SoMat Corporation system for its Strain Gauge Module is shown in Figure 55.9. It includes a power/processor/communication module, 1 MB CMOS extended memory unit, and eight strain gauge signal conditioning modules. The system is designed to collect strains through eight channels in both attended and unattended modes with a range of 2.1 to 12.5 mV. A second notebook computer is used to communicate with the SoMat system for commands regarding data acquisition mode, calibration, initialization, data display, and downloading of data. The SoMat system has been configured specifically for the purpose of collecting stress–strain histories and statistical analysis for highway bridges. This is possible due to the modular component arrangement of the system.

The data-acquisition system consists of five major components totaling 12 modules — eight strain transducer signal conditioning modules and four for Battery Pack, Power/Communications, 1-MB CMOS Extended Memory, and Model 2100 NSC 80180 Processor (see Figure 55.9). Regulated power is supplied by a rechargeable 11.3 to 13.4 V electrically isolated DC–DC converter. This unit powers all modules as well as provides excitation for strain transducers. Serial communications via RS 232C connector and battery backup for memory protection are provided by the Power/Communications

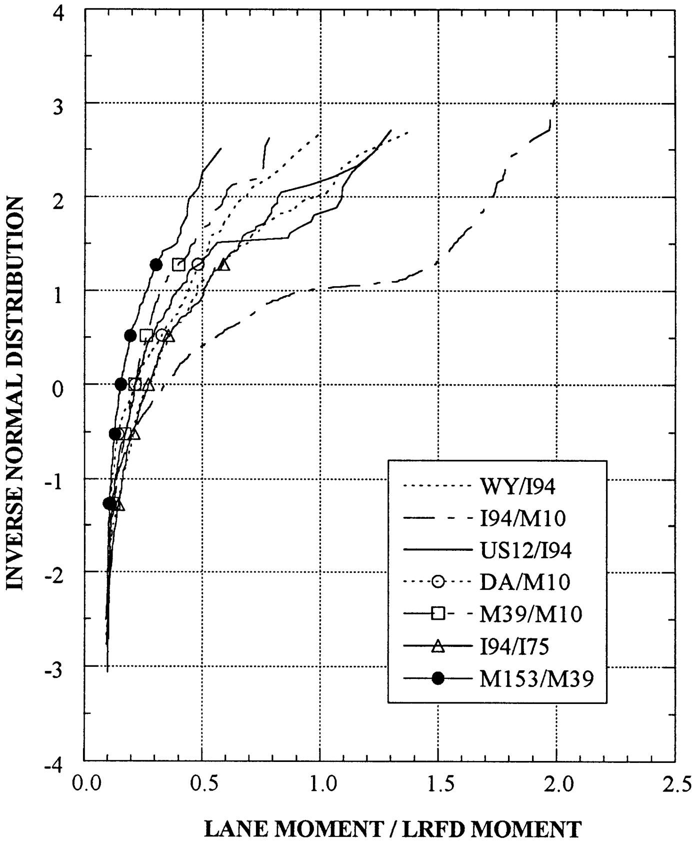

FIGURE 55.7 CDFs of lane moment for the span length of 27 m.

module. An Extended Memory Module of 1 Mbyte, high-speed, low-power CMOS RAM with backup battery for data protection is included for data storage. Eight strain gauge conditioning modules each provide 5-v strain transducer excitation, internal shunt calibration resistors, and an 8-bit, analog-to-digital converter.

Strain measurement range is ±2.1 mV minimum and ±12.5 mV maximum. The processor module consists of 32 kbytes of programmable memory and an NSC 80180 high-speed processor capable of sampling data in simultaneous mode resulting in a maximum sampling rate of 3000 Hz. Communication to the PC is via RS 232C at 57,600 baud. Data acquisition modes include time history, burst time history, sequential peak valley, time at level matrix, rainflow matrix, and peak valley matrix. Following collection, data are reviewed and downloaded to the PC hard drive for storage, processing, analysis, and plotting.

55.3.2 Rainflow Method of Cycle Counting

Development of a probabilistic fatigue load model requires collection of actual dynamic stress time histories of various members and components. Following the collection of time histories, data must be processed into a usable form. This section presents the characteristics of the dynamic stress time history commonly found in steel girder highway bridges as a random process, and rainflow method of counting fatigue damage.

Commonly occurring load histories in fatigue analysis often are categorized as either narrowband or wideband processes. Narrowband processes are characterized by an approximately constant period, such as that shown in Figure 55.10a. Wideband processes are characterized by higher

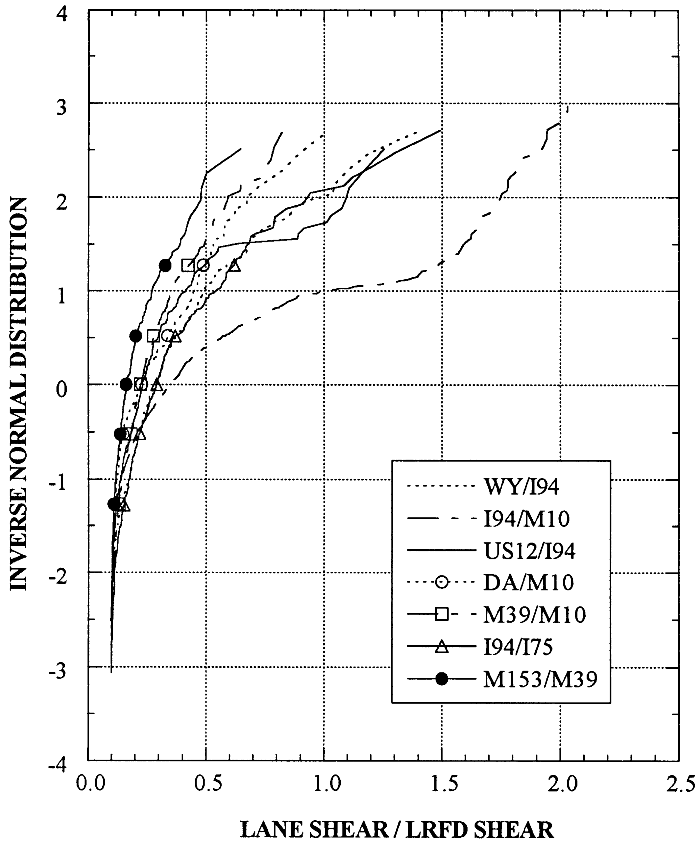

FIGURE 55.8 CDFs of lane shear for the span length of 27 m.

frequency small excursions superimposed on a lower, variable frequency process, such as that shown in Figure 55.10b. For steel girder highway bridges, where the loading is both random and dynamic, the stress histories are wideband in nature.

Stress histories that are wideband in nature do not allow for simple cycle counting. The cycles are irregular with variable frequencies and amplitudes. Several cycle-counting methods are available for the case of wideband and nonstationary processes, each successful to a degree in predicting the fatigue life of a structure. The rainflow method is preferred due to the identification of stress ranges within the variable amplitude and frequency stress histogram, which are associated with closed hysteresis loops. This is important when comparing the counted cycles with established fatigue test data obtained from constant-amplitude stress histories.

The rainflow method counts the number, n, of cycles in each predetermined stress range, S_i, for a given stress history. Rules of counting are applied to the stress history after orienting the trace vertically, positive time axis pointing downward. This convention facilitates the flow of "rain" due to gravity along the trace and is merely a device to aid in understanding of the method. Following are rules for the rainflow method (see Figure 55.11):

1. All positive peaks are evenly numbered.
2. A rainflow path is initiated at the inside of each stress peak and trough.
3. A rainflow progresses along a slope and "drips" down to the next slope.
4. A rainflow is permitted to continue unless the flow was initiated at a minimum more negative than the minimum opposite the flow and similarly for a rainflow initiated at a maximum. For example, path 1–8, 9–10, 2–3, 4–5, and 6–7.

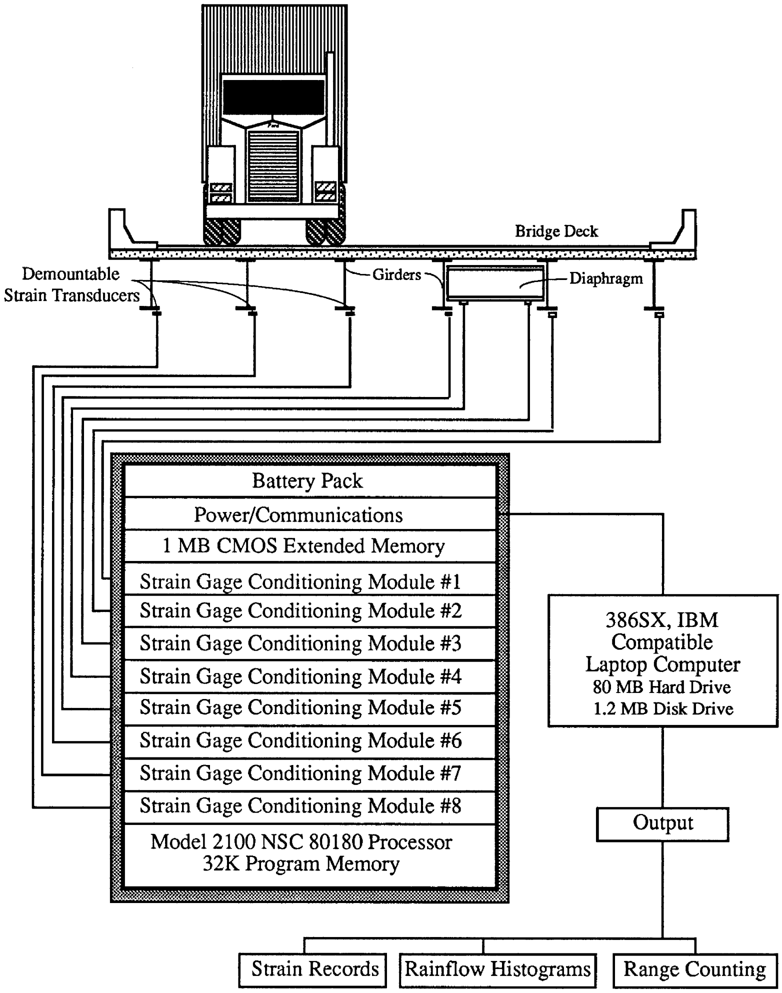

FIGURE 55.9 Somat strain data acquisition system.

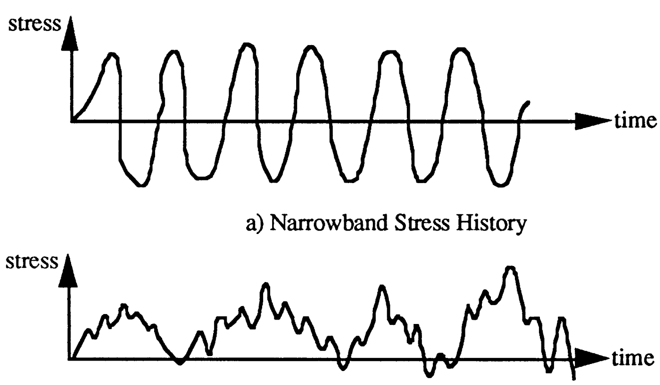

FIGURE 55.10 Example of narrowband (a) and wideband (b) stress histories.

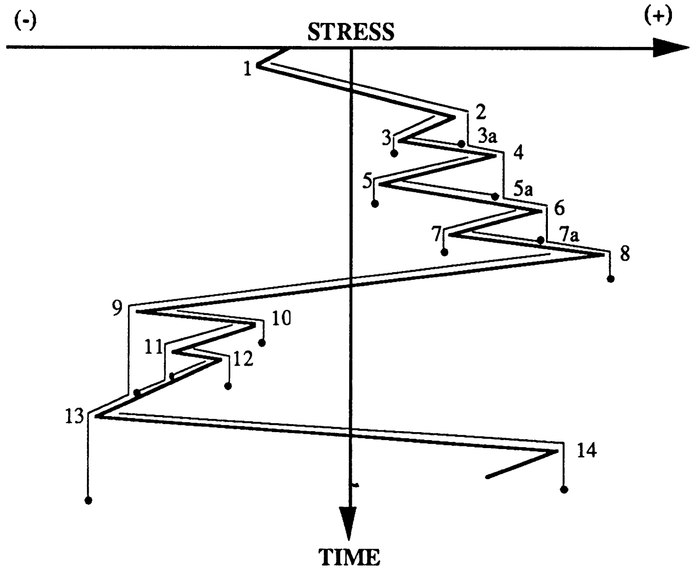

FIGURE 55.11 Rainflow counting diagram.

5. A rainflow must stop if it meets another flow that flows from above. For example, path 3–3a, 5–5a, and 7–7a.
6. A rainflow is not initiated until the preceding flow has stopped.

Following the above procedure each segment of the history is counted only once. Half cycles are counted between the most negative minimum and positive maximum, as well as the half cycles or interruptions between the maximum and minimum. As shown in Figure 55.11, all negative trough-initiated half cycles will eventually be paired with a peak initiated cycle of equal magnitude. For a more-detailed explanation and discussion of the rainflow method and others see an introductory text on fatigue analysis [9].

55.3.3 Results of Strain Spectra Testing

Strain histories were collected continuously for 1-week periods and reduced using the rainflow algorithm [5,6]. Data were collected for each girder in the bridge. The data are presented here in the form of CDFs and represent strain cycles due to 7 days of normal traffic. For an easier interpretation of results, the CDFs are plotted on normal probability paper (Figure 55.12).

For each bridge, the CDFs are shown for strains in girders numbered from 1 (exterior, on the right-hand side looking in the direction of the traffic). The number of girders for measured bridges varies from 6 to 10. The average strain is less than 50×10^{-6} for all girders and all bridges; however, the largest strains were observed in girders supporting the right traffic lane (girder numbers G3, G4, and G5) and nearest the left wheel of traffic in the right lane. As expected, the exterior girders of each bridge experience the lowest strain extremes in the spectrum.

As a means of comparison of fatigue live load, the equivalent stress, s_{eq}, is calculated for each girder using the following root mean cube (RMC) formula:

$$s_{eq} = \sqrt[3]{p_i S_i^3} \tag{55.1}$$

where S_i = midpoint of the stress interval i and p_i = the relative frequency of cycle counts for interval i. The stress, S_i, is calculated as a product of strain and modulus of elasticity of steel.

The CDFs of strain cycles and the corresponding equivalent stress values are shown in Figures 55.12 to 55.23. Stress values due to traffic load recorded in the girders are rather low. The maximum observed values are about 70 MPa. However, in most cases, the maximum values do not exceed 35 MPa for the most loaded girder, with most readings being about 7 MPa. Stress spectra considerably vary from girder to girder (component-specific). Therefore, the expected fatigue life is different depending on girder location. Exterior girders experience the lowest load spectra.

55.4 Dynamic Load Measurement

55.4.1 Introduction

The dynamic load is an important component of bridge loads. It is time variant, random in nature, and it depends on the vehicle type, vehicle weight, axle configuration, bridge span length, road roughness, and transverse position of trucks on the bridge. An example of the actual bridge response for a vehicle traveling at a highway speed is shown in Figure 55.24. For comparison, also shown is an equivalent static response, which represents the same vehicle traveling at crawling speed.

The dynamic load is usually considered as an equivalent static live load and it is expressed in terms of a dynamic load factor (DLF). There are different definitions for DLF, as summarized by Bakht and Pinjarkar [10] in their state-of-the-art report on dynamic testing of bridges. In this study, DLF is taken as the ratio of dynamic and static responses [7,11]:

$$\mathrm{DLF} = D_{\mathrm{dyn}}/D_{\mathrm{stat}} \tag{55.2}$$

where D_{dyn} = the maximum dynamic response (e.g., stress, strain, or deflection) measured from the test data, $D_{\mathrm{dyn}} = D_{\mathrm{total}} - D_{\mathrm{stat}}$; D_{total} = total response; and D_{stat} = the maximum static response obtained from the filtered dynamic response.

55.4.2 Measured Dynamic Load

Field measurements are performed to determine the actual truck load effects and to verify the available analytical models [7,11,12]. The tests are carried out on steel girder bridges. Measurements are taken using a WIM system with strain transducers. For each truck passage, the dynamic response is monitored by recording strain data. The truck weight, speed, axle configuration, and lane occupancy are also determined and recorded. A numerical procedure is developed to filter and process collected data. The DLF is determined under normal truck traffic for various load ranges and axle configurations.

An example of the actual static and dynamic stresses is shown in Figure 55.25. CDF of the static stress is plotted on the normal probability paper. For each value of static stress, the corresponding dynamic stress is also shown. The stress due to dynamic load is nearly constant and is not dependent on truck weight. Figure 55.26 shows DLFs as a function of static strains. Also shown in the figure is the power curve fit, which approximately represents mean values of DLFs. In general, the DLF decreases as the static strain increases. Therefore, the DLF is reduced for heavier trucks.

55.5 Summary

On the basis of WIM measurements, site-specific load spectra are presented for several bridge sites. Component stress spectra are presented for girders in the form of CDFs and the equivalent stresses are calculated for comparison. Site-specific statistics required for fatigue analysis based on current models are presented. Strains are measured to determine component-specific load spectra.

The truck load spectra for bridges are strongly site specific. Bridges located on major routes between large industrial metropolitan areas will experience the highest extreme loads. Routes where

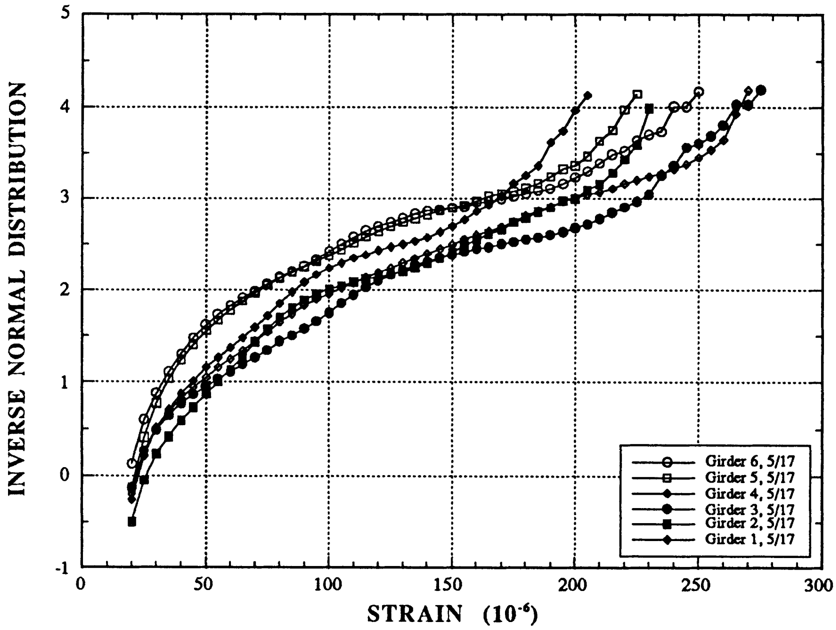

FIGURE 55.12 Strains for girders in bridge U.S. 23/HR.

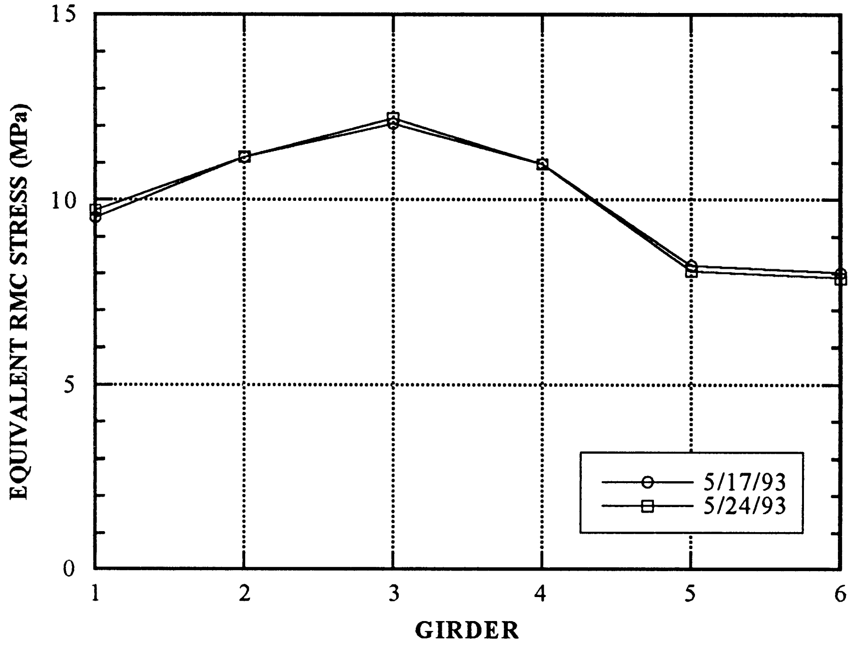

FIGURE 55.13 Equivalent stresses for girders in bridge U.S. 23/HR.

vehicles are able to circumvent stationary weigh stations will have very high extreme loads. Bridges not on a major route and those that are very near a weigh station experience lower extreme loads.

Live-load stress spectra are strongly component specific. Each component may have a different distribution of strain cycle range. The girder that is nearest the left wheel track of vehicles traveling

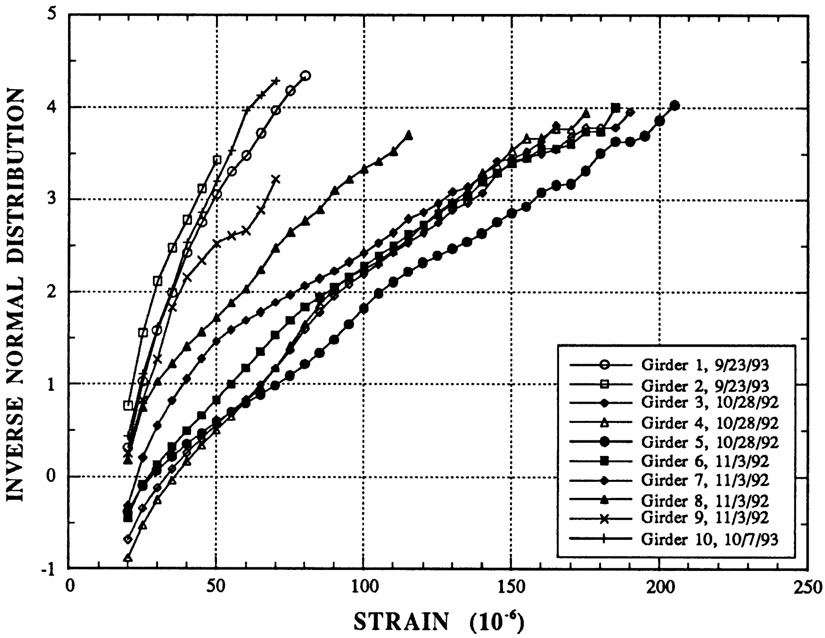

FIGURE 55.14 Strains for girders in bridge U.S. 23/SR.

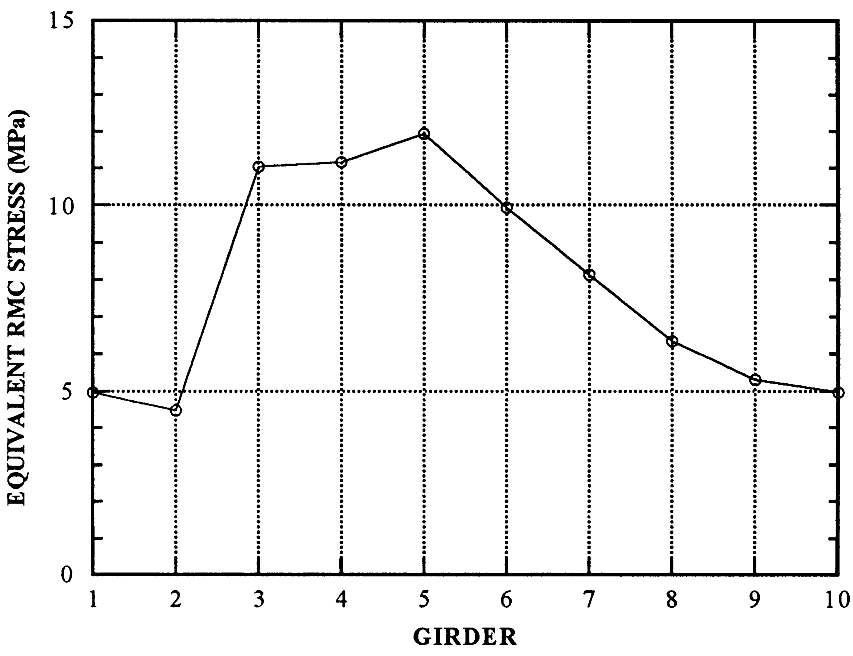

FIGURE 55.15 Equivalent stresses for girders in bridge U.S. 23/SR.

in the right lane experiences the highest stresses in the stress spectra. The stresses decrease as a function of the distance from this location. This information can be useful to target bridge inspection efforts to the critical members.

The stress due to dynamic load is nearly constant and it is not dependent on truck weight. In general, DLF decreases as the static strain increases. Therefore, the DLF is reduced for heavier trucks.

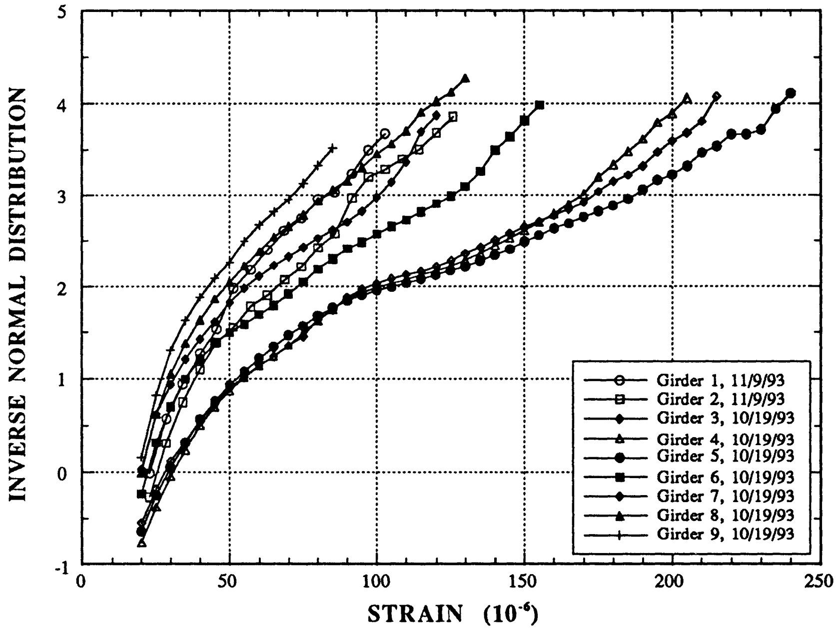

FIGURE 55.16 Strains for girders in bridge I-94/JR.

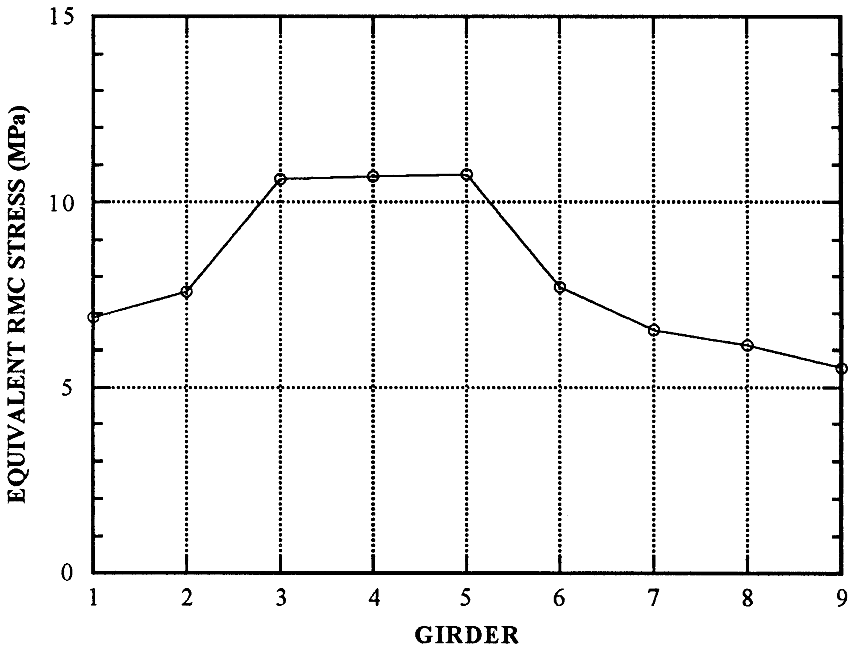

FIGURE 55.17 Equivalent stresses for girders in bridge I-94/JR.

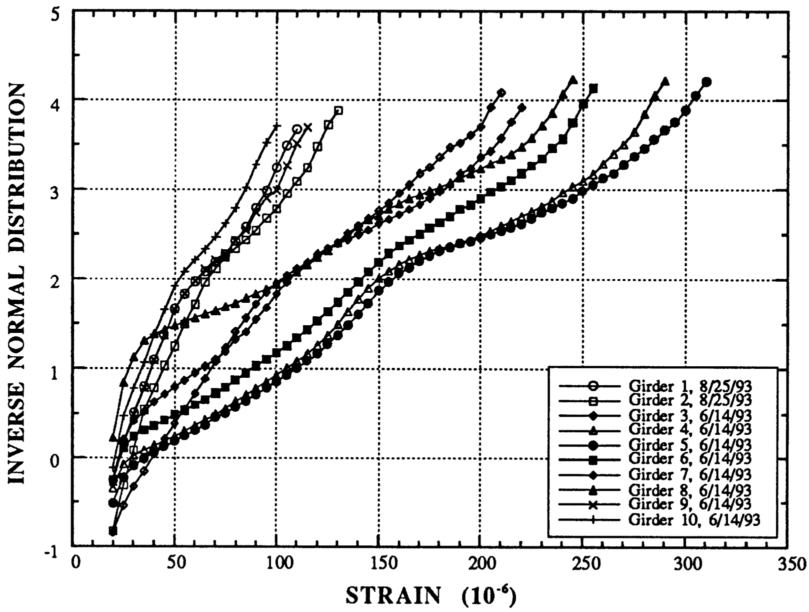

FIGURE 55.18 Strains for girders in bridge I-94/PR.

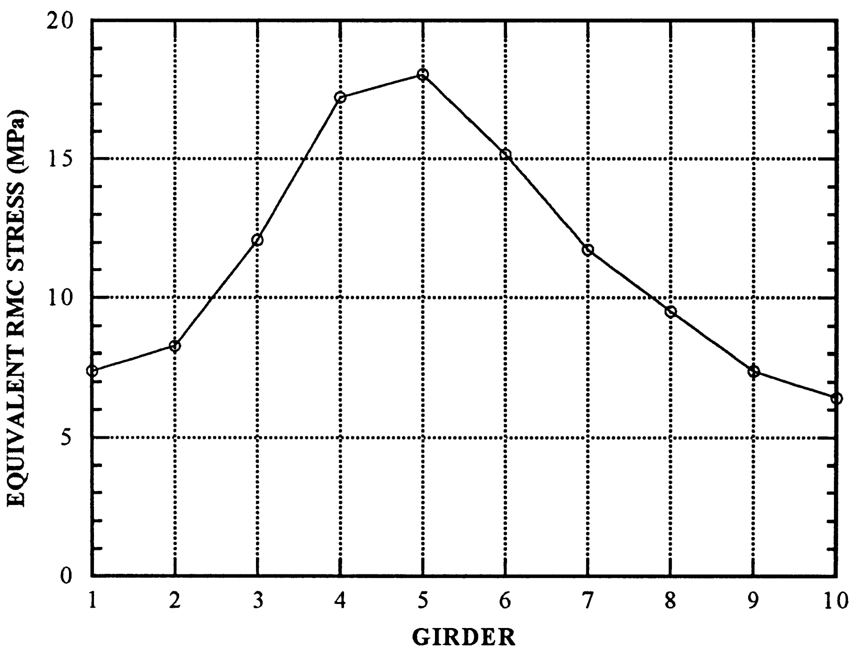

FIGURE 55.19 Equivalent stresses for girders in bridge I-94/PR.

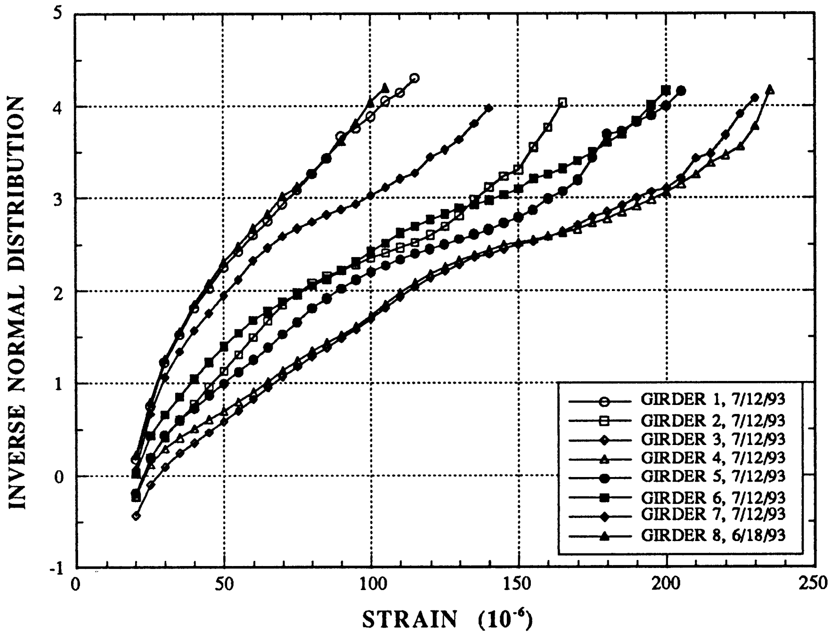

FIGURE 55.20 Strains for girders in bridge M-14/NY.

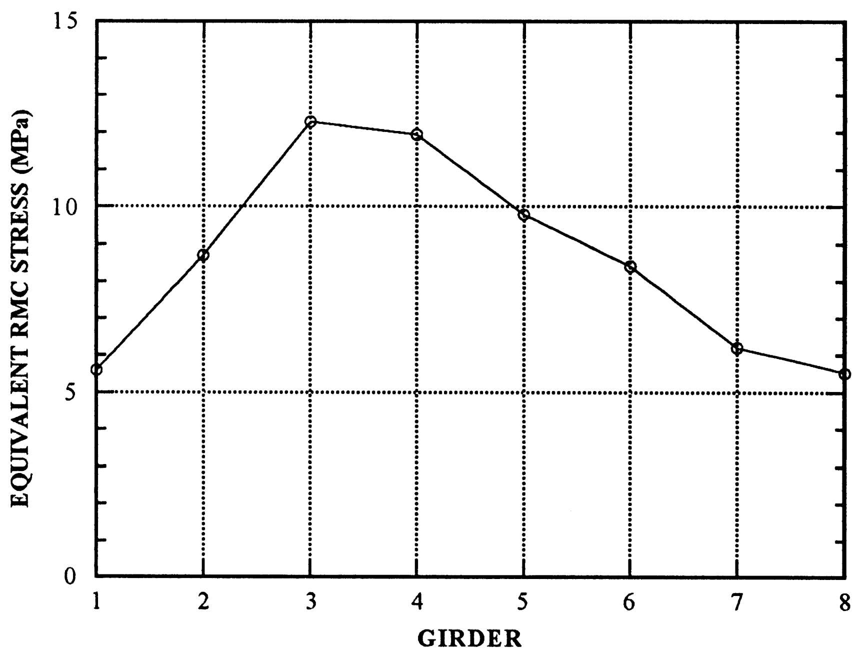

FIGURE 55.21 Equivalent stresses for girders in bridge M-14/NY.

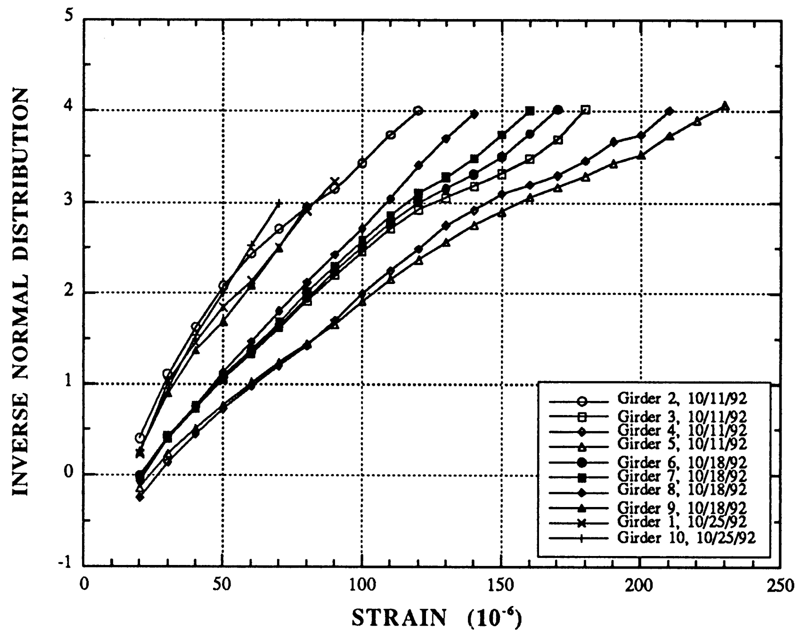

FIGURE 55.22 Strains for girders in bridge I-75/BC.

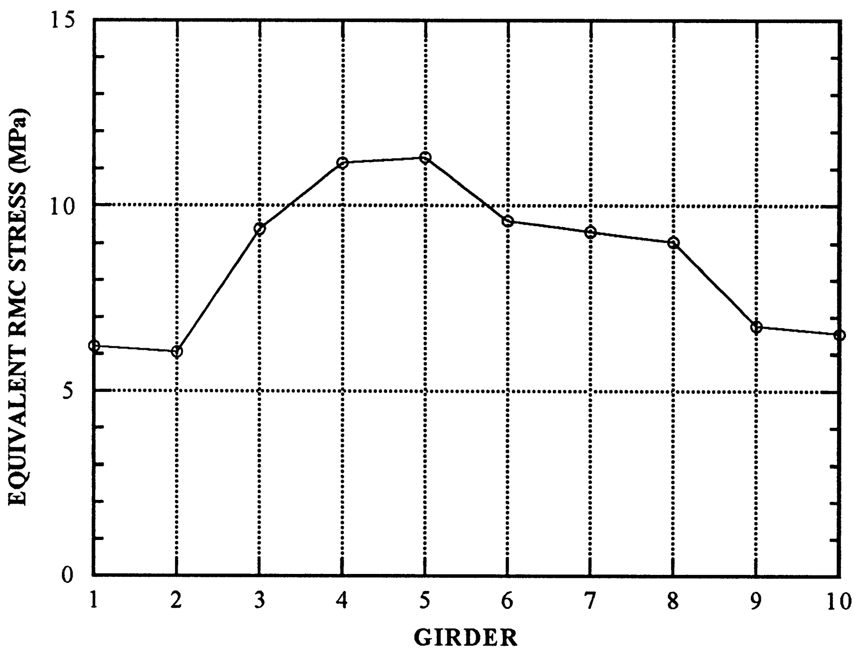

FIGURE 55.23 Equivalent stresses for girders in bridge I-75/BC.

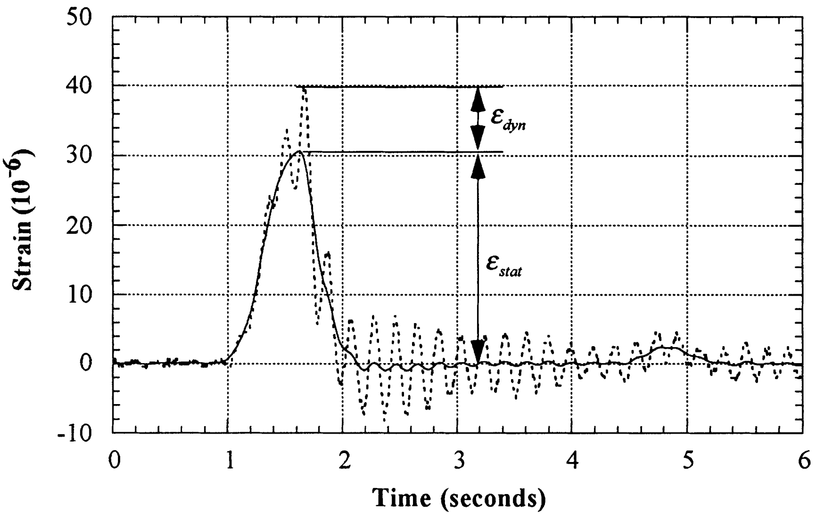

FIGURE 55.24 Dynamic and static strain under a truck traveling at highway speed.

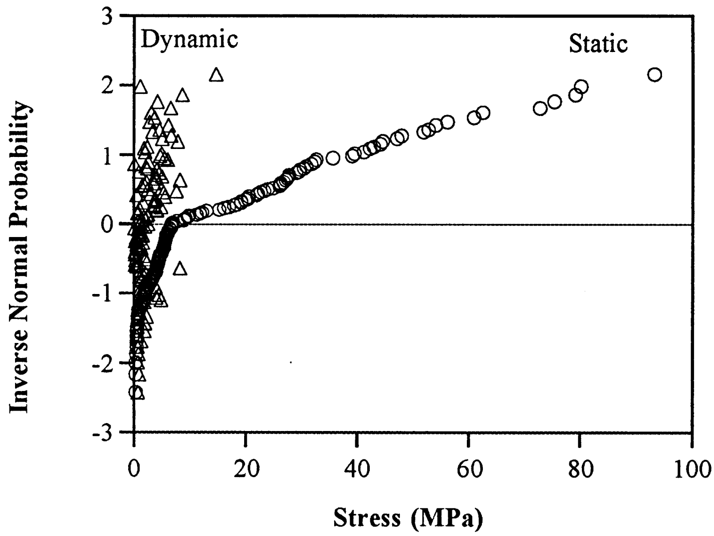

FIGURE 55.25 Typical CDF of static stress and corresponding dynamic stress.

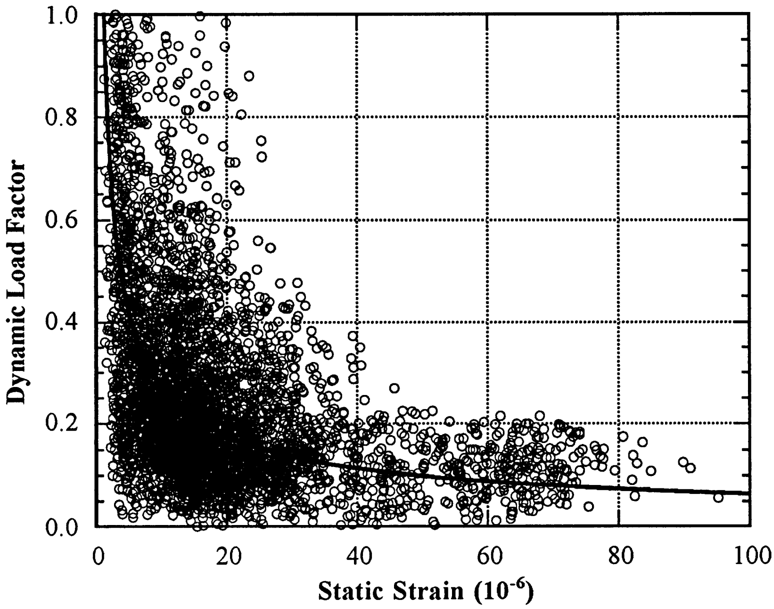

FIGURE 55.26 DLF vs. Static strain.

References

1. AASHTO, *LRFD Bridge Design Specifications*, 2nd ed., American Association of State and Transportation Officials, Washington, D.C, 1998.
2. Nowak, A. S. and Hong, Y-K., Bridge live-load models, *ASCE J. Struct. Eng.*, 117, 2757, 1991.
3. Kim, S., Sokolik, A. F., and Nowak, A. S., Measurement of truck load on bridges in the Detroit area, *Transp. Res. Rec.*, 1541, 58, 1996.
4. Nowak, A. S., Kim, S., Laman, J., Saraf, V., and Sokolik, A. F., Truck Loads on Selected Bridges in the Detroit Area, Research Report UMCE 94-34, University of Michigan, Ann Arbor, 1994.
5. Nowak, A. S., Laman, J. A., and Nassif, H., Effect of Truck Loading on Bridges, Report UMCE 94-22, Department of Civil and Environmental Engineering, University of Michigan, Ann Arbor, 1994.
6. Laman, J. A. and Nowak, A. S., Fatigue-load models for girder bridges, *ASCE J. Struct. Eng.*, 122, 726, 1996.
7. Kim, S. and Nowak, A. S., Load distribution and impact factors for I-girder bridges, *ASCE J. Bridge Eng.*, 2, 97, 1997.
8. Benjamin, J. R. and Cornell, C. A., *Probability, Statistics and Decision for Civil Engineers*, McGraw-Hill, New York, 1970.
9. Bannantine, J. A., Comer, J. J., and Handrock, J. L., *Fundamentals of Metal Fatigue Analysis*, Prentice-Hall, Englewood Cliffs, NJ, 1992.
10. Bakht, B. and Pinjarkar, S. G., Dynamic testing of highway bridges — a review, *Transp. Res. Rec.*, 1223, 93, 1989.
11. Nassif, H. and Nowak, A. S., Dynamic load spectra for girder bridges, *Transp. Res. Rec.*, 1476, 69, 1995.
12. Hwang, E. S. and Nowak, A. S., Simulation of dynamic load for bridges, *ASCE J. Struct. Eng.*, 117, 1413, 1991.